# Shadow Detection via Rayleigh Scattering and Mie Theory

Lin Gu[1] Antonio Robles-Kelly[1,2]
[1]College of Eng. and Comp. Sci., Australian National University, Canberra ACT 0200, Australia
[2]NICTA *, Locked Bag 8001, Canberra ACT 2601, Australia

## Abstract

*In this paper, we present a method to detect shadows in outdoor scenes. Here, we note that the shadow areas correspond to the diffuse skylight which arises from the scattering of the sunlight by particles in the atmosphere. This yields a treatment in which shadows in the image can be viewed as a linear combination of scattered light obeying Rayleigh scattering and Mie theory. This treatment allows for the computation of a ratio which permits casting the problem of recovering the shadowed areas in the image into a clustering setting making use of active contours. We illustrate the utility of the method for purposes of detecting shadows in real-world imagery and compare our results against a number of alternatives elsewhere in the literature.*

## 1. Introduction

Shadow detection and removal is an important preprocessing step for purposes of object recognition, video surveillance and segmentation [11]. This is particularly relevant in outdoor environments, where strong shadows ensue due to overcast conditions in addition to cast and self-shadowing.

Indeed, shadow detection has received ample attention in the computer vision community. For instance, in [13], a probabilistic method and matting are used to remove shadows based upon user input. In [12], a conditional Markov random field is used to detect shadows and perform background substraction in indoor scenes. In [8], the authors employ a Gaussian mixture model to characterise the moving cast shadows on the surfaces across the scene.

Despite recent interest, shadow detection in outdoor scenes remains a challenging task. Existing methods are often restricted to indoor environments [12], require prior knowledge regarding the illumination setting and geometry [6], employ multiple images [3] or require user input [13].

In this paper, we tackle the problem of detecting shadows in outdoor environments by viewing the shadowed areas in the image as being lit by skylight. This treatment permits the problem to be cast into a segmentation setting where active contour is used to detect the shadows in the image. The active contour evolution is governed by a ratio that arises from the use of Rayleigh scattering and Mie theory to model the skylight illuminating the shadowed areas.

The paper is organised as follows. In the following section, we model the skylight as a linear combination of the Rayleigh and Mie scattered light. With this linear combination at hand, we then present the ratio used for the evolution of the active contour, which we present in Section 4. We elaborate upon the implementation of our method in Section 5. Finally, we present results and conclusions in Sections 6 and 7.

## 2. Rayleigh Scattering and Mie Theory

Here, we note that, in outdoor scenes, the shadowed areas correspond to the diffuse skylight which arises from the scattering of the sunlight by particles in the atmosphere [9]. Thus, we can employ the Rayleigh scattering and Mie theory of sunlight propagation in the atmosphere to model the shadows. Recall that, when sunlight enters the atmosphere, it is scattered by the particles in the air. When these particles are small as compared to the wavelength of the impinging light, the scattering can be approximated by the proportion of the fourth power of the wavelength of the sun light, i.e. the Rayleigh scattering [5]. However, when the sunlight is scattered by particles bigger or of equal size to the wavelength, the phenomenon Mie theory [5], which states that the scattering is essentially independent of wavelength.

Thus, both, Mie theory and Rayleigh scattering must

*NICTA is funded by the Australian Government as represented by the Department of Broadband, Communications and the Digital Economy and the Australian Research Council through the ICT Centre of Excellence program.

be taken into account for modelling the skylight. This is as the air in the atmosphere will account for a large fraction of the Rayleght scattering whereas Mie theory is bound to apply to clouds and dust. Both the Rayleigh and Mie scattered light compose the skylight and, hence, we can write

$$E_{sky}(\lambda) = (1 - p_c)E_{rayleigh}(\lambda) + p_c E_{mie}(\lambda) \quad (1)$$

where, $\lambda$ is the wavelength parameter, $p_c$ is the contribution of the Mie scattering and $E_{mie}(\lambda)$ and $E_{rayleigh}(\lambda)$ corresponds to the Rayleigh scattered light.

## 3. Scattering Spectral Ratio

With the expression above, we can now turn our attention to the development of a ratio that can be used for purposes of separating the shadows in the imagery under consideration. Note that Rayleigh scattered light follows the proportion of the fourth power of the wavelength, i.e.

$$E_{rayleigh}(\lambda) = \frac{E(\lambda)}{\lambda^4}$$

whereas the Mie scattered light is independent of the wavelength, which implies

$$E_{mie} = \eta E(\lambda)$$

where $\eta$ is a proportionality constant. Thus, we have

$$E_{sky}(\lambda) \quad = \quad \left(\frac{1 - p_c}{\lambda^4} + p_c\eta\right)E(\lambda) \quad (2)$$

From Equation 2, we notice there is a linear relation between the non-scattered light $E(\lambda)$ and the sky light. This permits the use of a spectral ratio so as to describe the relation between the direct, i.e. non-scattered, light and the scattered skylight. The main advantage of this, as we will show later on, is that this ratio depends solely on the atmospheric conditions, such as humidity, cloud cover, etc.

To realise the importance of such observation, consider a diffuse shadowed image pixel $I_{shadow}(\lambda)$ and one of its neighbours $I_{direct}(\lambda)$ under direct illumination with the same surface reflectance $S(\lambda)$. These two pixels are, hence, illuminated by non-scattered light $E(\lambda)$ and skylight $E_{sky}(\lambda)$ such that their ratio satisfies the following relation

$$\frac{I_{shadow}(\lambda)}{I_{direct}(\lambda)} = \left(\frac{1 - p_c}{\lambda^4} + \eta p_c\right)\rho \quad (3)$$

where $\rho$ corresponds to the quotient between the shading factors for the two pixels under consideration. This follows from Equation 2 and the dichromatic model [10], where diffuse reflection is given by the product of the shading factor for the object surface, the illuminant and the material reflectance.

Note that $\rho$ can be removed from further consideration via the normalisation of the ratio in Equation 3. This yields

$$\varrho(\lambda) \quad = \quad \frac{\sum_\lambda I_{direct}(\lambda)^2}{\sum_\lambda I_{shadow}(\lambda)^2}\frac{I_{shadow}(\lambda)}{I_{direct}(\lambda)} \quad (4)$$

## 4. Active Contours

As mentioned earlier, to separate the shaded from the non-shaded regions in the image, we employ active contours. Active contours [1] are one of the most successful techniques in image segmentation. The basic idea is to evolve the contour for the boundary of the segmented region making use of constraints pertaining the problem in hand.

Thus, we use the active contour model in [16] with a level set function which makes use of the ratio $\varrho(\lambda)$ to construct the region-based signed pressure force function for the shadowed areas in the image. This shadow force pressure function controls the evolution of the contour so as to encourage shrinkage of the delimited area about the sunlit regions and expansion across shadowed regions. To define our shadow force pressure function, we use the pixel-wise ratio $\varrho(\lambda)$ and note that this should equate the value of

$$\zeta(p_c, \eta, \lambda) = \left(\frac{1 - p_c}{\lambda^4} + \eta p_c\right) \quad (5)$$

yielded by $p_c$ and $\eta$ as global image parameters. This is as $p_c$ and $\eta$ account for both, the atmospheric conditions and the proportion of Rayleigh and Mie scatterings across the scene. Our shadow pressure function $F(u)$ is given by

$$F(u) = \begin{cases} 1 & \text{if } \|\varrho(\cdot) - \zeta(p_c, \eta, \cdot)\| > \varepsilon \\ -1 & \text{if } \|\varrho(\cdot) - \zeta(p_c, \eta, \cdot)\| \leq \varepsilon \end{cases} \quad (6)$$

where $\varepsilon$ is a threshold value.

This yields the level set function of the form

$$\frac{\partial \phi}{\partial t} = F(u)\beta\|\nabla(\phi)\| \quad (7)$$

where $\beta$ is a parameter which governs the evolution speed of the contour.

## 5. Implementation Issues

In this section, we elaborate on the implementation issues regarding our algorithm. We commence by noting that, in our presentation above, we use $\zeta(p_c, \eta, \lambda)$ to

compute the force pressure function $F(u)$ for the pixel $u$. This assumes that both parameters, $p_c$ and $\eta$ are available. In practice, this is generally not the case. In our implementation, we estimate the value of $\zeta(p_c, \eta, \lambda)$ from the image itself.

We observe that the shadow boundaries should lie along the recovered edges. As a result, we use a Canny edge detector [2] so as to recover the edges in the image. For every pixel on these edges, we search its neighborhood and treat the highest intensity pixel as a directly illuminated one, whereas the lowest intensity pixel is viewed as the shadowed one. By assuming that the values of those $\varrho(\lambda)$ for the edge pixels in the image are normally distributed about $\zeta(p_c, \eta, \lambda)$, we can use the expected value, i.e. mean, over the ratios $\varrho(\lambda)$ for the edge pixels in the imagery as an estimator of $\zeta(p_c, \eta, \lambda)$. Thus, we have

$$\bar{\zeta}(\lambda) = \frac{1}{\mid \Omega \mid} \sum_{\Omega} \varrho(\lambda) \tag{8}$$

where $\Omega$ is the set of edge pixels in the image $\mathcal{I}$.

Also, note that, in the Section 3, we used a neighbour of the pixel $u$ to compute the corresponding ratio $\varrho(\lambda)$. To improve the robustness of the method to noise corruption and variations about the pixel $u$, we employ the ratio

$$\varrho_k^* = \frac{1}{\ell(u)} \sum_{q=\{R,G,B\}} I_q(u) \frac{\mid \mathfrak{N}_u \mid}{\sum_{v \in \mathfrak{N}_u} I_q(v)} \tag{9}$$

as an alternative to $\varrho(\lambda)$ in Equation 6.

In Equation 9, we have used $I_k(u)$ to denote the value for the colour channel $k = \{R, G, B\}$ at pixel $u$, $\ell(u)$ accounts for the pixel brightness and $\mathfrak{N}_u$ corresponds to the neighbourhood about the pixel $u$. We have done this since, in the previous sections we treated the problem in a general setting. This contrasts with our implementation, which aims at processing trichromatic imagery. Note that this can be done without any loss of generality since for a surface with reflectance $S(\lambda)$ illuminated by a light source a power spectrum $E(\lambda)$, the value of a diffuse pixel $u$ follows the relation [15]

$$I_k(u) = \int_{\Lambda_k} E(\lambda) S(\lambda) R(\lambda) d\lambda \tag{10}$$

where $R(\lambda)$ denotes the camera's colour sensitivity function over the operating wavelength range $\Lambda_k$ for each of the colour channels $k \in \{R, G, B\}$. This linear relation, compounded by the fact that we can recover $\zeta(p_c, \eta, \lambda)$ devoid of the reflectance making use of the pixel values allows for a similar treatment of Equation 8, where the colour channel index can be used as an alternative to the wavelength $\lambda$.

Finally, to set the initial shadow level set function, we divide the image into $M$ patches on a lattice and compute the ratio $\varrho_k$ (for the sake of consistency, we now use $k \in \{R, G, B\}$ as an alternative to $\varrho(\lambda)$) for each pair of patches using the mean of each patch. We set the shadow level set function $\nabla(\phi)$ to unity at the patches where the ratio is in better accordance with the estimated $\bar{\zeta}_k$ for each of the colour channels while setting $\nabla(\phi) = -1$ everywhere else. At each iteration of the level-set evolution, we regularize the shadow level set function with a Gaussian filter $G_\sigma$ with zero-mean and standard deviation $\sigma$.

## 6. Experiments

In this section we illustrate the utility of our method for purposes of shadow detection. To this end, we use a set of real-world images captured in the outdoors under a variety of atmospheric conditions making use of a Nikon D80. These vary from images with a large amount of cloud cover and high humidity to others with no clouds. In all our experiments, we have set the number $M$ of patches used for the initialisation of the level set function to $25 \times 25$, the neighbourhood $\mathfrak{N}_u$ is given by $15 \times 15$ pixels, the threshold $\epsilon$ is set to $0.3$ and the standard deviation of the Gaussian filter is $\sigma = 1$, the $\beta$ is set as 25.

In the Fig 1, we show the detection results for our algorithm and a number of alternatives. In this figure, the top row shows the detection results yielded by our method whereas the second and third rows show the result from the method in [7] and the algorithm presented in [4], respectively.

From the Fig 1, we can conclude that our method provides a margin of improvement over the alternatives, with the exception of the two shadows corresponding to the two tree canopies in the images on the second and fourth columns. It is worth noting in passing that, for these images, the boundary recovered by our method is consistent with the scattering theory used here, as these canopies act as a diffuser. Thus, these shadows are rather a mix of sunlight and skylight. Moreover, our method performs particularly well on the image in left-hand side column, where no other method can recover the shadows over the white paper. This is also evident in the third column, where the leaf in the middle of the shadow is classified by the methods in [7] and [4] as non-shadowed regions. Moreover, despite effective, the method in [7] does not necessarily deliver a closed shadow boundary. Note that this can potentially hinder shadow removal methods hinging in region filling or matting approaches, such as that in [14]. This is as the alternative aimed at detecting the shadow boundary.

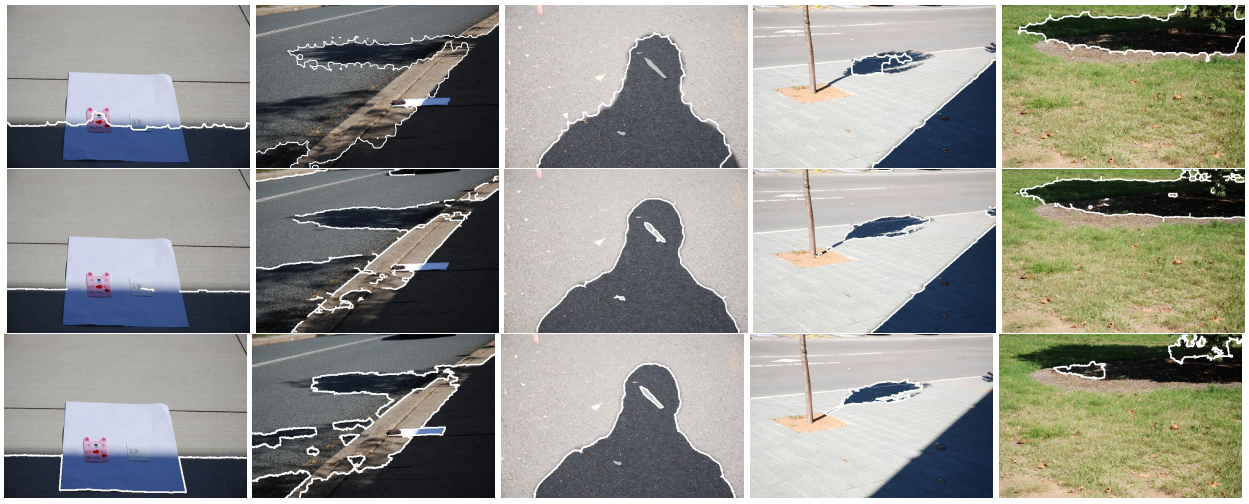

**Figure 1. Shadow detection results for our method and the alternatives.**

## 7. Conclusions

In this paper, we have presented a shadow detection method which hinges the use of Rayleigh scattering and Mie theory to model the skylight in outdoor imagery. We have shown how this treatment can be used to recover a ratio so as to govern the evolution of an active contour across the image. This allows for the shadow detection problem to be treated as a segmentation one. We have provided results on real-world imagery and compared our method against alternatives elsewhere in the literature.

## References


[1] A. Blake and M. Isard. *Active Contours: The Application of Techniques from Graphics, Vision, Control Theory and Statistics to Visual Tracking of Shapes in Motion*. Springer-Verlag, 1998.

[2] J. Canny. A computational approach to edge detection. *IEEE Trans. on Pattern Analysis and Machine Intelligence*, 8(6):679–698, 1986.

[3] G. Finlayson, S. Hordley, and M. S. Drew. Removing shadows from images. In *European Conf. on Comp. Vision*, pages 823–836, 2002.

[4] R. Guo, Q. Dai, and D. Hoiem. Single-image shadow detection and removal using paired regions. In *IEEE Conference on Computer Vision and Pattern Recognition*, 2011.

[5] M. Kerker. *The scattering of light, and other electromagnetic radiation*. Academic Press, 1969.

[6] D. C. Knill, D. Kersten, and P. Mamassian. Geometry of shadows. *J. Opt. Soc. Amer. A*, 14(12):3216–3232, 1997.

[7] J.-F. Lalonde, A. A. Efros, and S. G. Narasimhan. Detecting ground shadows in outdoor consumer photographs. In *European Conference on Computer Vision*, 2010.

[8] N. Martel-Brisson and A. Zaccarin. Moving cast shadow detection from a gaussian mixture shadow model. In *Computer Vision and Pattern Recognition*, pages 643–648, 2005.

[9] S. G. Narasimhan and S. K. Nayar. Vision and the atmosphere. *International Journal of Computer Vision*, 48(3):233–254, 2002.

[10] S. A. Shafer. Using color to separate reflection components. *Color Research and Applications*, 10(4):210–218, 1985.

[11] J. Tian, J. Sun, and Y. Tang. Tricolor attenuation model for shadow detection. *IEEE Transactions on Image Processing*, 18(10):2355–2363, 2009.

[12] Y. Wang, K. F. Loe, and J. K.Wu. Adynamic conditional random field model for foreground and shadow segmentation. *IEEE Trans. Pattern Anal. Mach. Intell.*, 28(2):279–289, 2006.

[13] T. P. Wu and C. K. Tang. A bayesian approach for shadow extraction from a single image. In *IEEE International Conference on Computer Vision*, page 480487, 2005.

[14] T. P. Wu, C. K. Tang, M. S. Brown, and H. Y. Shum. Natural shadow matting. *ACM Transactions on Graphics*, 26(2), 2007.

[15] G. Wyszecki and W. Stiles. *Color Science: Concepts and Methods, Quantitative Data and Formulae*. Wiley, 2000.

[16] K. Zhang, L. Zhang, H. Song, and W. Zhou. Active contours with selective local or global segmentation: A new formulation and level set method. *Image and Vision Computing*, 28(4):668–676, 2010.